

# A DYNAMIC CONTROLLER ARCHITECTURE FOR WHEELED MOBILE ROBOT TRAJECTORY TRACKING UTILIZING FEEDBACK LINEARIZATION AND STATE FEEDBACK

Anh-Minh Duc Tran<sup>1</sup>, Tri-Vien Vu<sup>2,\*</sup>

<sup>1</sup>Faculty of Electrical and Electronics Engineering, Ton Duc Thang University, Ho Chi Minh City, Vietnam.

<sup>2</sup>Modeling Evolutionary Algorithms Simulation and Artificial Intelligence, Faculty of Electrical and Electronics Engineering, Ton Duc Thang University, Ho Chi Minh City, Vietnam.

\*Corresponding Author: Tri-Vien Vu (email: vutrivien@tdtu.edu.vn)

(Received: 25-March-2024; accepted: 07-June-2024; published: 30-June-2024)

<http://dx.doi.org/10.55579/jaec.202482.456>

**Abstract.** *This paper presents a novel dual-loop trajectory tracking control strategy for differential-drive mobile robots (DDWMRs). The outer loop employs feedback linearization to address kinematic constraints and minimize position and heading errors. It generates control inputs for the inner loop, which utilizes state feedback control to manage the robot's dynamics. Actuator dynamics are incorporated to improve the model fidelity. The proposed system is implemented in MATLAB/Simulink. The uncertainty of the system is added to the model by using Uncertain State Space block. The proposed controller achieved high tracking accuracy for both circular and eight-shaped trajectories. In circular trajectories, the Relative-Root-Mean-Square-Error (RRMSE) remained below 7.2% (X-axis), 7.46% (Y-axis), and 3.16% (Yaw angle) over 3 seconds. Similarly, for eight-shaped trajectories, RRMSEs were approximately 5.25%, 8.19%, and 2.83% within 2 seconds. Simulation results demonstrate the robustness and effectiveness of the dual-loop controller in handling parameter uncertainties and achieving better trajectory tracking capability.*

**Keywords:** *Wheel Mobile Robot, MIMO, Feedback Linearization, State Feedback, Trajectory Tracking.*

## 1. Introduction

Because robots can do work with quality, accuracy, and efficiency, they are becoming a more prevalent substitute for humans in the real world. This is especially true in the fields of industry [1, 2], hospitality [3, 4], entertainment [5, 6] and the military [7]. The differential drive wheel mobile robot (DDWMR) is becoming more and more common among the various kinds of robots [8]. Unfortunately, a lack of the best controller in almost all DDWMRs produces inadequate results.

To accomplish the intended goals, several researchers have therefore suggested a variety of control frameworks. In [9], the authors suggested a unified tracking and regulation visual servoing strategy for a wheeled mobile robot with an onboard camera. The proposed unified controller exhibited asymptotic stability despite uncertainties in the object model and depth information, demonstrating its feasibility through both simulation and experimental results. Many attempts have been made [10] in order to present two control laws for trajectory tracking control

of non-holonomic mobile robots: quasi-sliding mode control for angular velocity and global terminal sliding mode control for linear velocity. Simulation results showed faster convergence of tracking errors for circular and sinusoidal reference trajectories, but the authors did not consider system dynamics in this paper. Nascimento and co-workers [11] hypothesized a novel approach for trajectory tracking control for nonholonomic mobile robots, using a nonlinear model predictive controller and modifications in the robot model, cost function, and optimizer to minimize steady-state error and address the issue of complex nonlinear vehicle dynamics. More recent evidence (Phuc *et. al.* [12]) revealed an adaptive fuzzy sliding mode control (AFSMC) for trajectory tracking control of a non-holonomic mobile robot system. The AF-SMC demonstrated strong resistance and the ability to handle parameter variation and system disturbance, eliminating chattering. Research has tended to focus on designing a dynamic controller for trajectory tracking control of DDWMRs, which may not be suitable and may result in reduced system performance due to the absence of actuator dynamics.

Much work has been done on DDWMR; however, the majority of the literature only addresses their kinematics models, which are appropriate for light-load, low-speed, and low-acceleration applications. When mobile robots operate at high speeds and carry large loads, the kinematic control loop cannot ensure precise velocity tracking. In order to reduce tracking errors, it becomes crucial to take robot dynamics into account. Furthermore, each side of the DDWMR chassis has its own independently driven wheel, which is powered by electric motors that may be adjusted separately in terms of speed and direction. The motors are coupled, resulting in DDWMR coupling multi-input-multi-output systems. This coupling issue is a prevalent problem in practice, complicating controller design.

This study considers both dynamic and kinematic model of DDWMR. Additionally, the dynamic model includes the actuators, which strengthens the DDWMR model's accuracy. Both inner loop and outer loop control strategies are introduced; the former utilizes state feedback

control to handle the dynamics of the system, while the latter employs feedback linearization method to control DDWMR kinematics.

The main contribution of this research is to improve the DDWMR model's accuracy by taking into account the system's actuator and applying the multiple input-multiple output (MIMO) model of DDWMR when designing the controller. The goal is to use the cascaded controller to obtain good trajectory tracking performance from the DDWMR in the presence of parameter uncertainty. The Uncertain State Space block, which is part of the block collection in the Robust Control Toolbox, is used to incorporate uncertainty information into Simulink models. It allows for the analysis of how variations in uncertainties affect system behavior and the evaluation of the robustness of the control approach being proposed. The performance of the suggested controller is evaluated using circular and eight-shape trajectories.

The remaining sections of the paper are organized as follows. Section 2. presents the derivation of the multivariable mathematical modeling of DDWMR. In Section 3. the design control techniques for the system are described. Section 4. discusses the simulation findings. Some conclusions are drawn in Section 5.

## 2. Modeling of system

The differential drive wheel mobile robot's kinematics, which consist of a stiff body and non-deforming wheels, are depicted in the schematic diagram in Figure 1, and the main notations used in this work are listed in Table 1 below. It is assumed that the mobile robot travels on a plane without slipping. On its platform, the DDWMR has one free castor wheel for balancing and two drive wheels with independent actuators positioned on the same axis. Controlling the respective angular velocities of the driving wheels allows the mobile robot to be navigated.

The proposed drive-wheeled model is fully integrated with two identical permanent magnet DC motors whose output shafts are coupled to corresponding driving wheels. The wheel hub

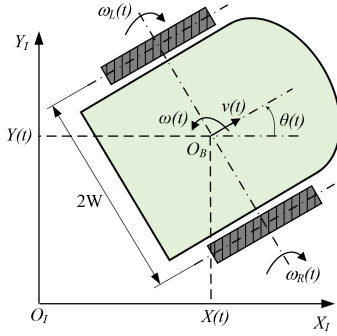


**Fig. 1:** Differential drive-wheeled mobile robot.

**Tab. 1:** Main notations for this work.

$v_R, v_L$	Linear speed of the right and left wheels
$\omega_R, \omega_L$	Angular speed of the right and left motors
$r_W$	Radius of the wheels
$i_G$	Gearbox ratio of the motors
$\nu$	Longitudinal velocity of the DDWMR
$\omega$	Angular velocity of the DDWMR
$2W$	Distance from the right-to-left wheel's ground contact point
$\nu_X, \nu_Y$	X and Y-axis velocities of the DDWMR
$\theta$	Orientation of the DDWMR
$i_{aR}, i_{aL}$	Armature current of the right and left DC motors
$u_{aR}, u_{aL}$	Armature voltage of the right and left DC motors

centers' longitudinal speeds are established by

$$\nu_L = \frac{r_W}{i_G} \omega_L \text{ and } \nu_R = \frac{r_W}{i_G} \omega_R \quad (1)$$

At the midpoint of the line connecting the wheel hub centers, the DDWMR's longitudinal velocity  $\nu$  and yaw rate  $\omega$  are

$$\begin{aligned} \nu &= \frac{1}{2} (\nu_R + \nu_L) = \frac{r_W}{2i_G} (\omega_R + \omega_L) \\ \omega &= \frac{1}{2W} (\nu_R - \nu_L) = \frac{r_W}{2Wi_G} (\omega_R - \omega_L) \end{aligned} \quad (2)$$

The linear and angular velocities of DDWMR in the inertial frame are stated as follows [13]:

$$\begin{aligned} \nu_X &= \nu \cos \theta \\ \nu_Y &= \nu \sin \theta \\ \dot{\theta} &= \omega \end{aligned} \quad (3)$$

The dynamic model of the DDWMR in state space form is provided by [14] when the actuators and robot system are treated according to

Newton's second law:

$$\begin{aligned} \dot{\mathbf{x}} &= \mathbf{Ax} + \mathbf{Bu} \\ \mathbf{y} &= \mathbf{Cx} \end{aligned} \quad (4)$$

where,

$$\mathbf{A} = \begin{bmatrix} -k_{1R} & -k_{2R} & 0 & 0 \\ k_{4R} & -k_{5R} & -k_{6R} & k_{7R} \\ 0 & 0 & -k_{1L} & -k_{2L} \\ -k_{6L} & k_{7L} & k_{4L} & -k_{5L} \end{bmatrix},$$

$$\mathbf{B} = \begin{bmatrix} k_{3R} & 0 \\ 0 & 0 \\ 0 & k_{3L} \\ 0 & 0 \end{bmatrix}, \mathbf{C} = \begin{bmatrix} 0 & k_{8R} & 0 & k_{8L} \\ 0 & k_{9R} & 0 & -k_{9L} \end{bmatrix}$$

In this model  $\mathbf{x} = [i_{aR} \ \omega_R \ i_{aL} \ \omega_L]^T$ ,  $\mathbf{y} = [\nu \ \omega]^T$ ,  $\mathbf{u} = [u_{aR} \ u_{aL}]^T$  are states, output, and input vectors, respectively. Our earlier work has specifics regarding the modeling and simulation of each component [14].

### 3. Controller design

In this study, the design and structure of the trajectory tracking controller are separated into two stages. Using the errors between the desired position  $[X_{ref} \ Y_{ref} \ \theta_{ref}]^T$  and the actual robot position  $[X \ Y \ \theta]^T$ , the kinematic controller is first utilized to generate the desired linear and angular velocities. The second stage is the design of the dynamic controller, which is utilized to compensate for the mobile robot's dynamic effects. Figure 2 illustrates the trajectory tracking controller's whole architecture.

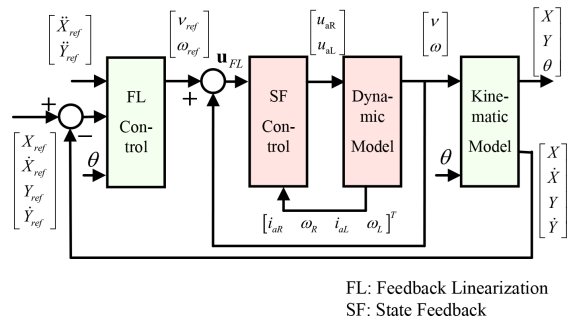


**Fig. 2:** Overall trajectory tracking controller of DDWMR.

### 3.1. Feedback linearization control for trajectory tracking of DDWMR

By introducing a transformation to the system input, feedback linearization aims to achieve a linear system between new input and output [15]. This makes it possible to develop any linear control system. In line with the kinematic model, their initial derivative is

$$\begin{cases} \dot{X} = \nu_X = \nu \cos \theta \\ \dot{Y} = \nu_Y = \nu \sin \theta \end{cases} \quad (5)$$

Only the translational velocity  $\nu$  is shown in the first derivative. The second derivative is

$$\begin{cases} \ddot{X} = \dot{\nu} \cos \theta - \nu \dot{\theta} \sin \theta \\ \ddot{Y} = \dot{\nu} \sin \theta + \nu \dot{\theta} \cos \theta \end{cases} \quad (6)$$

Both of the velocities  $\nu$  and  $\omega = \dot{\theta}$  are included in Equation 6. Currently, the system of equations is reformulated such that the functions of the highest derivatives of individual inputs ( $\dot{\nu}$  and  $\omega$ ) describe the second derivatives of the flat outputs.

$$\begin{bmatrix} \ddot{X} \\ \ddot{Y} \end{bmatrix} = \begin{bmatrix} \cos \theta & -\nu \sin \theta \\ \sin \theta & \nu \cos \theta \end{bmatrix} \begin{bmatrix} \dot{\nu} \\ \omega \end{bmatrix} = \mathbf{F} \begin{bmatrix} \dot{\nu} \\ \omega \end{bmatrix} \quad (7)$$

It is now possible to introduce the non-singular matrix  $\mathbf{F}$  if  $\nu = 0$ . Thus, the system of equations can be solved for  $\dot{\nu}$  and  $\omega$ :

$$\begin{bmatrix} \dot{\nu} \\ \omega \end{bmatrix} = \mathbf{F}^{-1} \begin{bmatrix} \ddot{X} \\ \ddot{Y} \end{bmatrix} = \begin{bmatrix} \cos \theta & \sin \theta \\ -\frac{1}{\nu} \sin \theta & \frac{1}{\nu} \cos \theta \end{bmatrix} \begin{bmatrix} \ddot{X} \\ \ddot{Y} \end{bmatrix} \quad (8)$$

The recently acquired linear system comprises inputs  $[u_{FL1} \ u_{FL2} \ t]^T = [\ddot{X} \ \ddot{Y}]^T$ , and states  $\mathbf{z} = [X \ \dot{X} \ Y \ \dot{Y}]^T$ . The state-space model provides a straightforward way to characterize the dynamics of the new system is

$$\begin{bmatrix} \dot{X} \\ \ddot{X} \\ \dot{Y} \\ \ddot{Y} \end{bmatrix} = \begin{bmatrix} 0 & 1 & 0 & 0 \\ 0 & 0 & 0 & 0 \\ 0 & 0 & 0 & 1 \\ 0 & 0 & 0 & 0 \end{bmatrix} \begin{bmatrix} X \\ \dot{X} \\ Y \\ \dot{Y} \end{bmatrix} + \begin{bmatrix} 0 & 0 \\ 1 & 0 \\ 0 & 0 \\ 0 & 1 \end{bmatrix} \begin{bmatrix} u_{FL1} \\ u_{FL2} \end{bmatrix} \quad (9)$$

or

$$\dot{\mathbf{z}} = \mathbf{A}_{FL}\mathbf{z} + \mathbf{B}_{FL}\mathbf{u}_{FL} \quad (10)$$

Since the controllability matrix of the system in Equation 10 has a complete rank, the state feedback controller for every given characteristic polynomial of the closed loop exists, indicating that the system is controllable.

Another necessity is to create the control law so that the robot follows a reference trajectory. In the context of flat systems, a reference trajectory for flat outputs is presented as  $X_{ref}(t)$ ,  $Y_{ref}(t)$ .

Then the reference can be retrieved for the system state  $\mathbf{z}_{ref} = [X_{ref} \ \dot{X}_{ref} \ Y_{ref} \ \dot{Y}_{ref}]^T$  and the system input  $\mathbf{u}_{FLref} = [\ddot{X}_{ref} \ \ddot{Y}_{ref}]^T$ . Equation 10 can alternatively be expressed for reference signals:

$$\dot{\mathbf{z}}_{ref} = \mathbf{A}_{FL}\mathbf{z}_{ref} + \mathbf{B}_{FL}\mathbf{u}_{FLref} \quad (11)$$

Errors between the actual and reference states is characterized as  $\tilde{\mathbf{z}} = \mathbf{z} - \mathbf{z}_{ref}$ . Subtracting Equation 11 from Equation 10 results in

$$\dot{\tilde{\mathbf{z}}} = \mathbf{A}_{FL}\tilde{\mathbf{z}} + \mathbf{B}_{FL}(\mathbf{u}_{FL} - \mathbf{u}_{FLref}) \quad (12)$$

Equation 12 defines the dynamics of the state error. These dynamics should be steady and appropriately quick. One method for regulating closed-loop dynamics is to specify closed-loop pole locations. As demonstrated previously, the pair  $(\mathbf{A}_{FL}, \mathbf{B}_{FL})$  is controlled; thus, it is possible to attain arbitrary placements of the closed-loop poles in the left half-plane of the complex plane  $s$  by appropriately choosing a constant control gain matrix  $\mathbf{K}_{FL}$  (of dimension  $2 \times 4$ ). It is possible to rewrite the equation 12 as follows:

$$\begin{aligned} \dot{\tilde{\mathbf{z}}} &= (\mathbf{A}_{FL} - \mathbf{B}_{FL}\mathbf{K}_{FL})\tilde{\mathbf{z}} + \mathbf{B}_{FL}\mathbf{K}_{FL}\tilde{\mathbf{z}} + \mathbf{B}_{FL}(\mathbf{u}_{FL} - \mathbf{u}_{FLref}) \\ &= (\mathbf{A}_{FL} - \mathbf{B}_{FL}\mathbf{K}_{FL})\tilde{\mathbf{z}} + \mathbf{B}_{FL}(\mathbf{K}_{FL}\tilde{\mathbf{z}} + \mathbf{u}_{FL} - \mathbf{u}_{FLref}) \end{aligned} \quad (13)$$

If the final part in Equation 13,  $(\mathbf{K}_{FL}\tilde{\mathbf{z}} + \mathbf{u}_{FL} - \mathbf{u}_{FLref})$  is zero, the state errors converge to 0 with the prescribed dynamics, provided by the matrix  $(\mathbf{A}_{FL} - \mathbf{B}_{FL}\mathbf{K}_{FL})$  of the closed-loop system. The control law for this method is defined by forcing this term to zero:

$$\begin{aligned} \mathbf{u}_{FL}(t) &= -\mathbf{K}_{FL}\tilde{\mathbf{z}}(t) + \mathbf{u}_{FLref}(t) \\ &= -\mathbf{K}_{FL}[\mathbf{z}(t) - \mathbf{z}_{ref}(t)] + \mathbf{u}_{FLref}(t) \\ &= \mathbf{K}_{FL}[\mathbf{z}_{ref}(t) - \mathbf{z}(t)] + \mathbf{u}_{FLref}(t) \end{aligned} \quad (14)$$

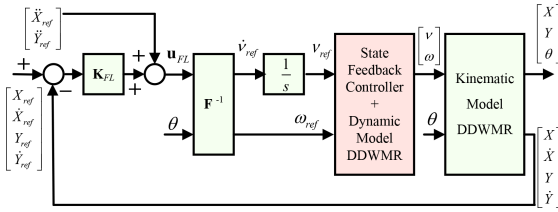


**Fig. 3:** Feedback linearization for reference tracking.

Because of a particular type of matrix  $\mathbf{A}_{FL}$ ,  $\mathbf{B}_{FL}$  in Equation 9, where  $u_{FL1}$  only influences states  $Z_1, Z_2$ , while  $u_{FL2}$  only influences states  $Z_3, Z_4$  the controller gain matrix is:

$$\mathbf{K}_{FL} = \begin{bmatrix} k_{FL1} & k_{FL2} & 0 & 0 \\ 0 & 0 & k_{FL3} & k_{FL4} \end{bmatrix} \quad (15)$$

Thus, the control law Equation 14 may be expressed as follows:

$$\begin{aligned} u_{FL1}(t) &= \ddot{X}(t) = k_{FL1} [X_{ref}(t) - X(t)] + k_{FL2} [\dot{X}_{ref}(t) - \dot{X}(t)] + \ddot{X}_{ref}(t) \\ u_{FL2}(t) &= \ddot{Y}(t) = k_{FL3} [Y_{ref}(t) - Y(t)] + k_{FL4} [\dot{Y}_{ref}(t) - \dot{Y}(t)] + \ddot{Y}_{ref}(t) \end{aligned} \quad (16)$$

### 3.2. State feedback for dynamic control of DDWMR

Examine the state-variable model provided in Equation 4

$$\begin{aligned} \dot{\mathbf{x}} &= \mathbf{Ax} + \mathbf{Bu} \\ \mathbf{y} &= \mathbf{Cx} \end{aligned} \quad (17)$$

The controller must be designed to allow tracking of a step reference input with zero steady-state error, which is a design challenge. In this paper, the reference input is  $\mathbf{r} = [\nu_{ref} \ \omega_{ref}]^T$  and the tracking error  $\mathbf{e}$  is

$$\mathbf{e} = \mathbf{r} - \mathbf{y} \quad (18)$$

Finding the time derivative yields

$$\dot{\mathbf{e}} = \dot{\mathbf{r}} - \dot{\mathbf{y}} = -\mathbf{C}\dot{\mathbf{x}} \quad (19)$$

According to [16], the two intermediary variables are defined as follows:

$$\begin{cases} \mathbf{q} = \dot{\mathbf{x}} \\ \mathbf{w} = \dot{\mathbf{u}} \end{cases} \quad (20)$$

then

$$\begin{bmatrix} \dot{\mathbf{e}} \\ \dot{\mathbf{q}} \end{bmatrix} = \begin{bmatrix} \mathbf{0} & -\mathbf{C} \\ \mathbf{0} & \mathbf{A} \end{bmatrix} \begin{bmatrix} \mathbf{e} \\ \mathbf{q} \end{bmatrix} + \begin{bmatrix} \mathbf{0} \\ \mathbf{B} \end{bmatrix} \mathbf{w} \quad (21)$$

If Equation 21 is controllable, we can obtain feedback control law in the following form:

$$\mathbf{w} = -\mathbf{K}_1 \mathbf{e} - \mathbf{K}_2 \mathbf{q} \quad (22)$$

such that Equation 21 is stable. This suggests a stable tracking error  $\mathbf{e}$ , and hence the goal of asymptotic tracking with zero steady-state error is accomplished. Integrating Equation 22 yields the control input, which is

$$\mathbf{u} = -\mathbf{K}_1 \int_0^t \mathbf{e}(\tau) d\tau - \mathbf{K}_2 \mathbf{x} \quad (23)$$

The corresponding block diagram of the state feedback control algorithm is shown in Figure 4.

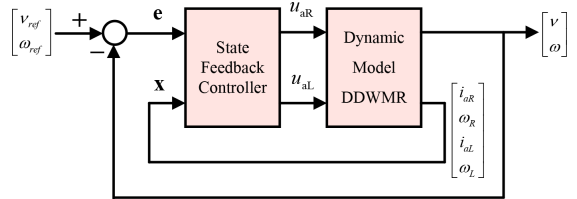


**Fig. 4:** Pole placement with integral control block diagram.

## 4. Results and discussions

The effectiveness of the suggested control strategy is assessed in this section both with and without parameter uncertainty. This section assesses the suggested control method's performance in two scenarios: one in which parameter uncertainty exists and the other in which it does not. The Simulink model of the DDWMR using the state feedback method for dynamic control and feedback linearization control for trajectory tracking is displayed in Figure 5. The parameters of the system are listed in Table 2 below.

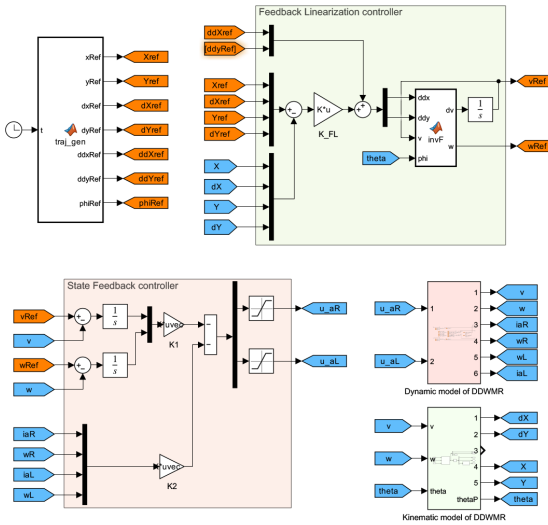


**Fig. 5:** Simulink model of the overall trajectory tracking controller of DDWMR.

**Tab. 2:** Specifications of the DDWMR.

Symbol	Description	Value	Units
$J_Z$	Moment of inertia of DDWMR	0.35	kg.m <sup>2</sup>
$m_B$	Mass of DDWMR	15	kg
$W$	Half wheel base length	0.2	m
$m_W$	Wheel mass	0.5	kg
$J_W$	Moment of inertia of wheel	0.0002	kg.m <sup>2</sup>
$i_G$	Gearbox ratio	2	-
$\eta_G$	Gearbox efficiency	85	%
$r_W$	Wheel radius	0.0675	m
$B_m$	Motor viscous coefficient	0.0132	N.ms/rad
$K_t$	Motor torque constant	0.6303	N.m/A
$L_a$	Armature winding inductance	0.0172	H
$R_a$	Armature winding resistance	0.7424	$\Omega$

### 4.1. Trajectory tracking

#### Case Study 1: Circular path

To evaluate the suggested controller’s tracking capability, a circular reference trajectory for the DDWMR is chosen for the simulation.

$$\begin{aligned} X_{ref} &= 0.5 + 0.7 \cos(2\pi t/30) \\ Y_{ref} &= 0.3 + 0.7 \sin(2\pi t/30) \end{aligned} \tag{24}$$

The simulation time for trajectory tracking in this case is 30 seconds to ensure the robot finishes one period. The robot’s initial position is at (0.8, 0), while the reference trajectory starts at (1.2, 0.3). The performance response of the circular reference trajectory tracking is displayed in Figure 6 As can be seen in the fig-

ure, the real trajectory can track the reference trajectory after a short time.

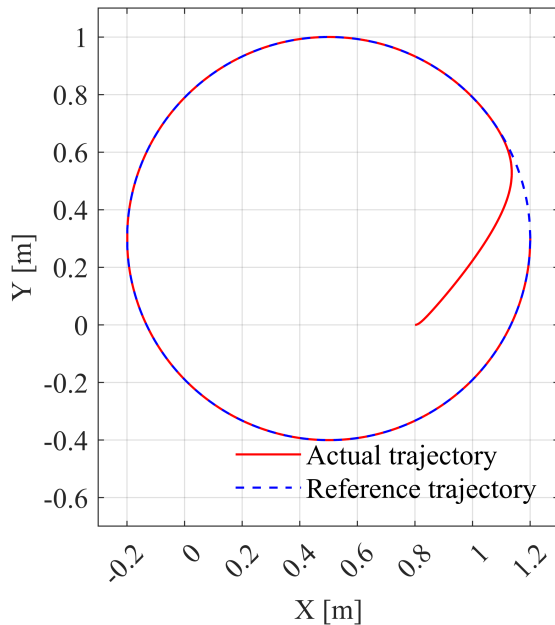


**Fig. 6:** Circular trajectory tracking.

The position and orientation tracking errors of the mobile robot under the operation of the proposed controllers are shown in Figure 7 The X and Y-position tracking errors start at 0.4 and 0.3, respectively, and then converge to almost zero within 2 seconds. Meanwhile, the orientation tracking error starts at an initial error of 1.57 and gradually decreases to zero over a relatively long time of approximately 3 seconds.

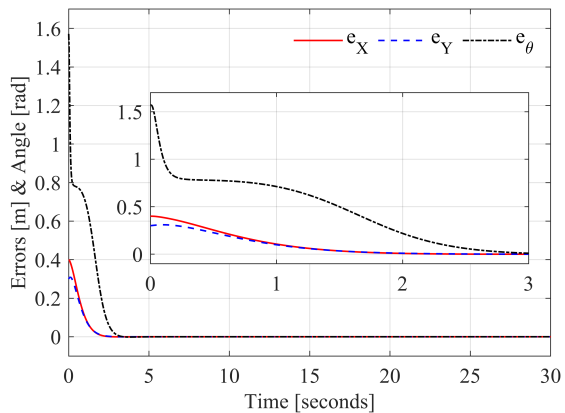


**Fig. 7:** Position and orientation tracking errors.

To evaluate the tracking capability, the Relative-Root-Mean-Square-Error (RRMSE) is used as a metric. The RRMSE is defined by

$$\text{RRMSE} = \frac{\sqrt{\frac{1}{n} \sum_{i=1}^n (y_{D,i} - y_{A,i})^2}}{\sqrt{\frac{1}{n} \sum_{i=1}^n y_{D,i}^2}} \cdot 100 \quad (25)$$

where  $n$  is the number of data points,  $y_{D,i}$  is the desired output and  $y_{A,i}$  is the actual output value.

The RRMSE in X-, Y-axis, and orientation are 7.2%, 7.46%, and 3.61%, respectively. The corresponding control inputs are the armature voltages applied to the right and left wheel motors, as shown in Figure 8. Since the reference trajectory is a circular path with a fixed radius, the desired left and right motor angular speeds will be constants. As a result, in a steady state, the voltages applied to the right and left motors will be constant.

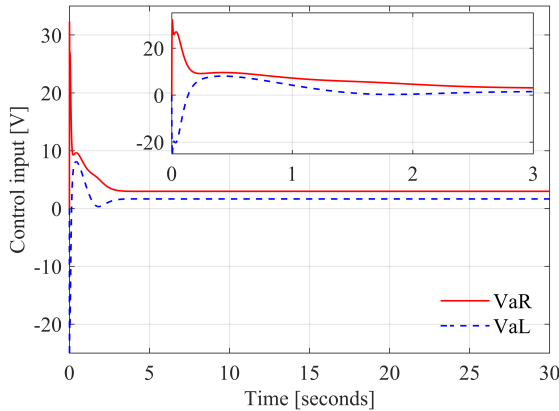


Fig. 8: Control input for right and left wheel motors.

### Case study 2: Eight-shape reference trajectory

In this case study, the performance of the proposed system is evaluated with an eight-shape reference trajectory defined by:

$$\begin{aligned} X_{ref} &= 0.5 + 0.7 \sin(2\pi t/30) \\ Y_{ref} &= 0.3 + 0.7 \sin(4\pi t/30) \end{aligned} \quad (26)$$

Assuming that the robot initiates at (0.2, 0) and the reference trajectory begins at (0.5, 0.3), the

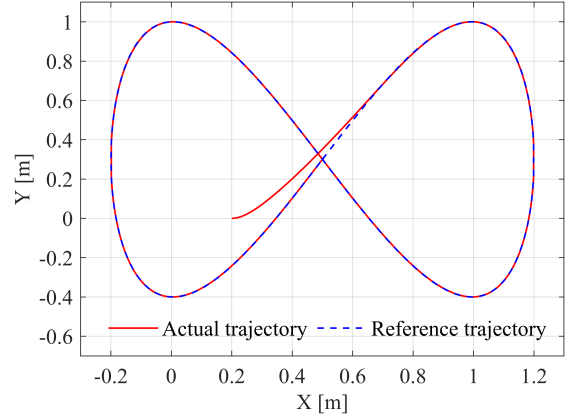


Fig. 9: Eight-shape-type trajectory tracking.

simulation duration for following the trajectory in this scenario is 30 seconds.

The tracking performance is shown in Figure 9 and the corresponding errors are shown in Figure 10. It can be seen that after less than two seconds, the tracking errors for both positions and orientation asymptotically approach zeros. The corresponding RRMSEs are approximately 5.25%, 8.19%, and 2.83%, respectively. In this case study, the control inputs for the right and left wheel motors are as shown in Figure 11.

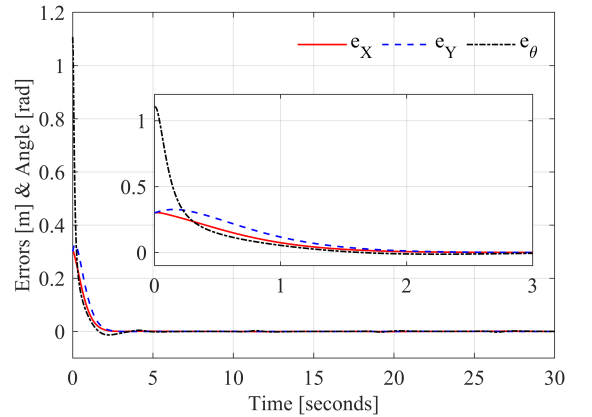


Fig. 10: Position and orientation tracking errors.

## 4.2. Parameter variations

The trajectory tracking algorithm consistently requires a DDWMMR model. However, due to the inability to precisely measure the physical

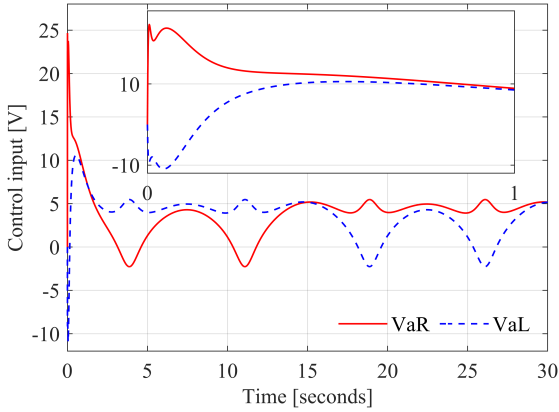


Fig. 11: Control input for right and left wheel motors.

parameters, the controller is designed using the nominal value of these parameters. Nevertheless, when the algorithm is implemented on an actual model, the true value of DDWMR may deviate from the nominal value parameters chosen in the algorithm, thereby unavoidably impacting the algorithm’s control effectiveness. In this study, the variation of the eight parameters: radius of the wheel  $r_W$ , efficiency of the motor  $\eta_G$ , wheel mass  $m_W$ , wheel inertia  $J_W$ , motor armature winding resistance  $R_a$ , motor armature winding resistance  $L_a$ , motor torque constant  $K_t$  and motor viscous coefficient  $B_m$  on each side of DDWMR is specifically taken into account due to practical considerations. These parameters are taken to be constants, but there could be a 10% relative uncertainty around the nominal values. In order to examine the impact of uncertainty on the model’s responses, the Simulink model will incorporate uncertain real parameters using the MATLAB command ‘ureal’ [17]. The MATLAB command ‘usample’ will then be employed to generate random values for these parameters. Additionally, the command ‘ufind’ will be used to identify the ‘uncertain state space blocks’ within the Simulink model and compile a comprehensive list of all uncertain variables present in these blocks.

Analyze the step response of the open-loop system using the MATLAB ‘step’ command to understand the behavior that the uncertainty represents. This command mechanically generates a series of random samples from an uncertain system. A collection of step responses illus-

trates the plant variability is shown in Figure 12. This figure illustrates the step responses of the armature voltage of the left and right DC motors to the longitudinal and angular velocities of the DDWMR’s dynamic model. The graphics display the response of the nominal system as a solid red line, while the responses of the uncertain system are represented by dashed blue lines. The simulation results indicate that the nominal value of  $\nu$  (from  $u_{aR}$ ) is 0.0317 and it ranges from 0.0271 to 0.0372. Similarly, the nominal value of  $\omega$  (from  $u_{aR}$ ) is 0.159 and it also ranges from 0.138 to 0.186. Additionally, characteristics rise time and settling time, ... also deviate significantly from the nominal value, which poses challenges in precisely controlling the trajectory of DDWMR.

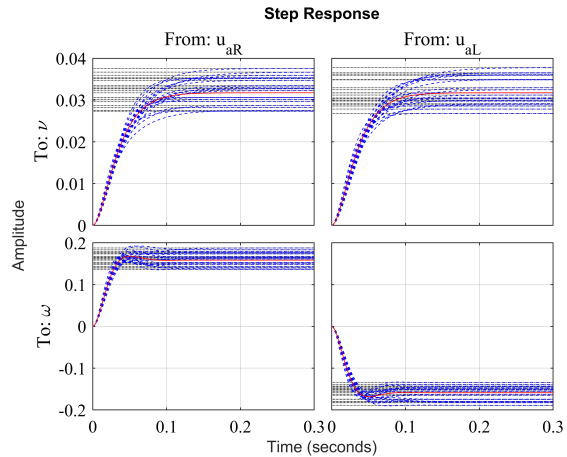
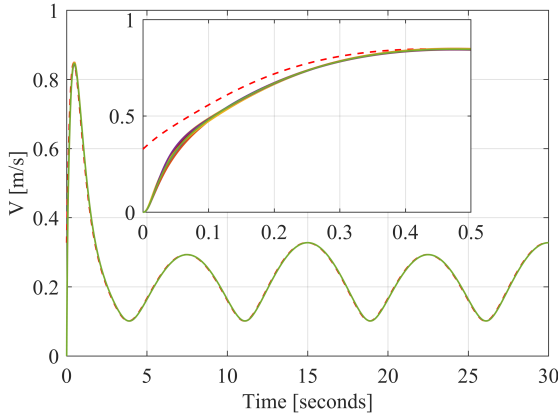


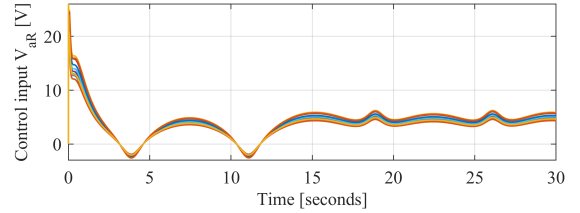
Fig. 12: Step responses of uncertain open-loop dynamic system.

The longitudinal velocity and yaw rate transient responses of the uncertain closed-loop system in the test with the eight-shape trajectory are shown in Figure 13 and Figure 14. In these figures, the dashed red line is the reference signal, and the remaining lines are the response signals. The simulation results show that after a period of about 0.5 seconds, the response lines follow the reference signal. The transient responses of the actual positions and heading angle also closely match the desired signal.

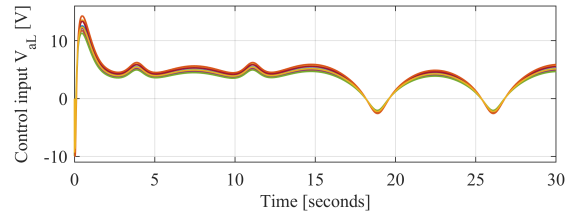
It can be seen that the DDWMR model’s parameter uncertainty can be compensated by the proposed controller. The efficacy of the con-



**Fig. 13:** Closed-loop transient response of DDWMR's longitudinal velocity.



(a) Right wheel motor



(b) Left wheel motor

**Fig. 15:** Control inputs.

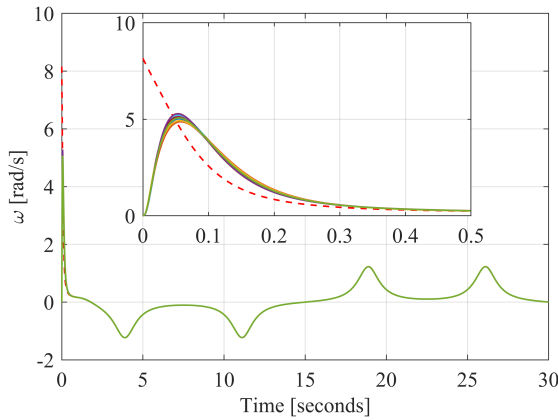


**Fig. 14:** Closed-loop transient response of DDWMR's yaw rate.

troller in adapting control signals to account for variations in model parameters during simulations is seen in Figure 15. Simulating the behavior of the system with uncertain parameters when the trajectory is in the shape of a circle also yields similar results. The variation in the RRMSE of responses can be seen in Figure 16.

## 5. Conclusions

This study proposes a novel dual-loop control strategy for DDWMRs. It combines feedback linearization for precise kinematic control with state feedback control to ensure robust dynamic response. The controller's performance was rigorously evaluated in simulations using various

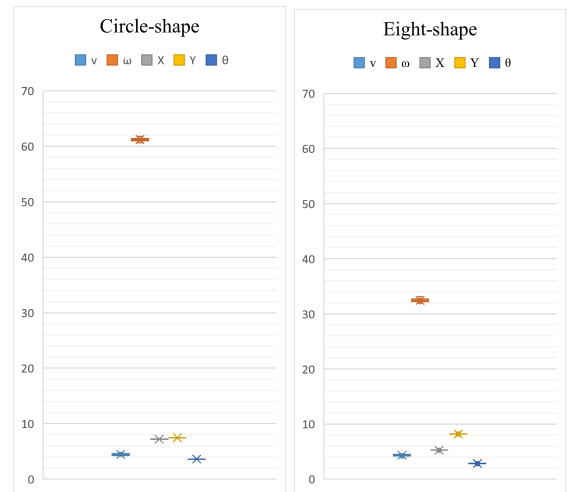


**Fig. 16:** Variation of RRMSE for parameter uncertainty.

metrics, including settling time and relative-root-mean-square error (RRMSE). It achieved excellent tracking accuracy for both circular and eight-shaped trajectories, with low RRMSE values. Furthermore, simulations incorporating parameter uncertainty via Simulink's Uncertain State Space block confirmed the controller's stability. These findings suggest the proposed dual-loop controller's potential for real-world applications with strict tracking requirements and uncertain operating conditions.

## References

- [1] C. Takva and Z.Y. Ilerisoy. Flying robot technology (drone) trends: A review in the building and construction industry. *Archit. Civ. Eng. Environ.*, 16:47–68, 2023.
- [2] R. Bogue. Robots in the offshore oil and gas industries: a review of recent developments. *Ind. Robot: international journal robotics research application*, 47:1–6, 2020.
- [3] H. Park, S. Jiang, O.K.D Lee, and Y. Chang. Exploring the attractiveness of service robots in the hospitality industry: analysis of online reviews. *Inf. Syst. Front.*, 26:41–61, 2024.
- [4] W. Ladeira, M.G. Perin, and F. Santini. Acceptance of service robots: a meta-analysis in the hospitality and tourism industry. *J. Hosp. Mark. & Manag.*, 32:694–716, 2023.
- [5] R. Bogue. The role of robots in entertainment. *Ind. Robot: international journal robotics research application*, 49:667–671, 2022.
- [6] K.J. Morris, V. Samonin, J. Baltes, J. Anderson, and M.C. Lau. A robust interactive entertainment robot for robot magic performances. *Appl. Intell.*, 49:3834–3844, 2019.
- [7] S. Swethaa and A. Felix. An intuitionistic dense fuzzy ahp-topsis method for military robot selection. *J. Intell. & Fuzzy Syst.*, 44:6749–6774, 2023.
- [8] C. Rosmann, F. Hoffmann, and T. Bertram. Integrated online trajectory planning and optimization in distinctive topologies. *Robotics Auton. Syst.*, 88:142–153, 2017.
- [9] B. Li, Y. Fang, G. Hu, and X. Zhang. Model-free unified tracking and regulation visual servoing of wheeled mobile robots. *IEEE Trans. on Control. Syst. Technol.*, 24:1328–1339, 2015.
- [10] W. Benaziza, N. Slimane, and A. Malle. Mobile robot trajectory tracking using terminal sliding mode control. *6th Int. Conf. on Syst. Control.*, pages 538–542, 2017.
- [11] T.P. Nascimento, C.E. Dórea, and L.M. Gonçalves. Nonlinear model predictive control for trajectory tracking of nonholonomic mobile robots: A modified approach. *Int. J. Adv. Robotic Syst.*, 15:1729881418760461, 2018.
- [12] P.T. Phuc, T.P. Tho, N.D. Hai, and N.T. Thinh. Design of adaptive fuzzy sliding mode controller for mobile robot. *Int. J. Mech. Eng. Robotics Res.*, 10:54–59, 2021.
- [13] T.V Vu, A.M.D Tran, B.H. Nguyen, and H.V.V Tran. Development of decentralized speed controllers for a differential drive wheel mobile robot. *J. Adv. Eng. Comput.*, 7:76–94, 2023.
- [14] A.M.D. Tran and T.V. Vu. A study on general state model of differential drive wheeled mobile robots. *J. Adv. Eng. Comput.*, 7:174–186, 2023.
- [15] G. Klancar, A. Zdesar, S. Blazic, and I. Skrljanc. Wheeled mobile robotics: from fundamentals towards autonomous systems. *Butterworth-Heinemann*, 2017.
- [16] R.C. Bishop. Modern control systems. *Pearson*, 2016.
- [17] G. Balas, R. Chiang, A. Packard, and M. Safonov. Robust control toolbox user's guide. *The Math Work. Inc., Tech. Rep.*, 2024.

## About Authors

**Tri-Vien VU** Received the B.Eng. degree in mechatronics from Hanoi University of Science and Technology Ha Noi, Vietnam, in 2005, and the M.Sc. and Ph.D. degrees from Da-yeh University, Changhua, Taiwan in 2011 and 2015, respectively, all in mechanical and automation engineering. He joined the Faculty Electrical and Electronics Engineering, Ton Duc Thang University, Ho Chi Minh City, Vietnam, and work as a Lecturer since 2015. His research interests include vehicle dynamic, mobile robot, power electronics, electrical drives.

**Anh Minh D. TRAN** got his B.S.

and M.S. degrees in Control and Automation Engineering from Ho Chi Minh City University of Transport in 2008 and Ho Chi Minh University of Technology in 2013, respectively, and his Ph.D. from Pukyong National University in Busan, Korea, in 2017. He is currently a lecturer at the Faculty of Electrical and Electronics Engineering at Ton Duc Thang University in Ho Chi Minh City, Vietnam. His scientific interests include control theory, computer vision, vehicle dynamics, and mobile robots with applications to industry and the environment. He can be contacted by email at [tranducanhminh@tdtu.edu.vn](mailto:tranducanhminh@tdtu.edu.vn).